Electronics and Electrical Engineering

AIMS Electronics and Electrical Engineering, 10(3): 473–503
DOI: 10.3934/electreng.2026019
Received: 28 February 2026
Revised: 28 April 2026
Accepted: 15 May 2026
Published: 10 June 2026

https://www.aimspress.com/journal/ElectrEng

Research article

Leader-follower formation control of quadcopter UAVs using a Mamdani fuzzy PID controller with performance evaluation under disturbance conditions

Vo Van An*

Institute of Engineering Technology, Thu Dau Mot University, Ho Chi Minh City, Vietnam

* **Correspondence:** Email: anvv@tdmu.edu.vn; Tel: +84942048086.

Abstract: This paper proposes and evaluates a triangular formation control method for unmanned aerial vehicles (UAVs) based on a leader-follower structure using a Mamdani fuzzy PID controller on a fully nonlinear 6-DOF dynamic model. The controller was designed with a fuzzy inference mechanism to adjust PID gains via a rule-based, nonlinear fuzzy gain-scheduling mechanism based on state deviations, thereby improving trajectory tracking quality under nonlinear conditions and disturbances. The system's performance was evaluated through transient metrics and energy error indicators (MSE, RMSE) in three scenarios: no noise, external noise, and external noise combined with wind disturbance. Simulation results in MATLAB/Simulink showed that under noise-free conditions, the fuzzy PID achieves a rise time of 2.03 s, a percentage overshoot of 50.30%, and a steady-state error of 0.0315 m, significantly improving upon the PID (3.29 s; 55.74%; 0.0365 m). When external noise is present, the overshoot decreases from 227.50% to 88.58%, and the steady-state error decreases from 1.0272 to 0.4060 m (approximately 60.5% improvement). In conditions with combined wind disturbance, MSE decreases by up to 87.49% along the z-axis, and RMSE decreases from 1.1538 to 0.4081, demonstrating superior disturbance rejection. Quantitative results confirm that fuzzy PID significantly enhances trajectory tracking accuracy, stability, and robustness of the multi-agent UAV system in uncertain environments.

Keywords: PID; fuzzy PID; leader-follower; UAV swarm; disturbance

1. Introduction

In recent years, unmanned aerial vehicles (UAVs), especially quadcopter UAVs, have been widely applied in monitoring, search and rescue, cargo transportation, environmental observation, and military missions. Modern trends not only focus on single control but also extend to formation control, where multiple UAVs coordinate to maintain a defined geometric structure to enhance coverage, flexibility, and system fault tolerance.

However, UAV formation control is a challenging problem due to the strong nonlinearity of the 6-DOF dynamic model, the coupling between translational and rotational motion, and the influence of environmental noise, such as wind, and model discrepancies. Classical control methods, such as traditional proportional-integral-derivative (PID), are often insufficient to handle the nonlinearities, uncertainties, and interactions in the dynamics of multi-UAV systems [1–5]. In contrast, fuzzy logic control (FLC) provides a rule-based reasoning mechanism suitable for highly nonlinear and uncertain systems [8,9]. Researchers have extensively investigated a wide range of advanced control strategies to enhance UAV formation performance, including linear quadratic regulator (LQR) [6], nonlinear robust control [7], backstepping control [10,11], fuzzy PID control [12,13], optimal control [14,15], model predictive control (MPC) [16], sliding mode control (SMC) [17–19], and neural network-based control [20,21], as well as methods combining PID with integral state feedback [22]. Recently, intelligent and data-driven approaches, such as fault diagnosis using hybrid deep learning, adaptive fuzzy systems with time-varying delays, and AI-based control models, have shown great potential in enhancing the robustness, adaptability, and fault tolerance of systems in complex dynamic environments [23–29]. These studies emphasize the importance of selecting an appropriate control structure to ensure stability, robustness, and high performance for UAV systems operating under uncertain conditions.

Recent studies have focused on developing and implementing control solutions to enhance trajectory tracking efficiency and maintain a stable UAV formation, especially in the leader-follower model [30–34]. In [30], a formation control method was proposed based on the relative pose relationship between the leading and following UAVs. This method combines sliding mode control with backstepping and a PID controller that adapts its structure, thereby improving convergence speed and control accuracy. The authors in [31] exploited cooperative control principles to design a PID controller for multi-agent UAV systems. Based on the system model and the communication structure among UAVs, the controller was optimized to minimize tracking errors and achieve rapid convergence to the desired trajectory. In [32], the problem was addressed experimentally, implementing formation control for two Parrot AR Drone 2.0 UAVs using a linear system model that accounts for delays. Researchers have designed a PD controller using the pole placement method to ensure stable position tracking. The system operates in various modes, in which the following UAV adjusts its position based on information from the leading UAV, with results quantified by an RMSE index that fluctuates between 50 and 115 cm. Using a numerical simulation approach, the study in [33] developed a formation control framework based on a UAV model implemented in MATLAB/Simulink. Algorithms such as LQR, PID, and MPC were implemented and compared in terms of performance based on position and formation structure criteria. Additionally, the algorithm incorporated factors such as the azimuth angle and the distance between UAVs to maintain accurate orientation. Meanwhile, the study [34] focused on UAV formation control in environments with obstacles by combining model predictive control (MPC) and artificial potential field (APF) algorithms. This solution not only ensured

continuous target tracking but also maintained geometric formation (square or hexagonal) after overcoming both static and dynamic obstacles, demonstrating the effectiveness and flexibility of the proposed method in complex situations.

Although substantial research on UAV formation control has been conducted, several significant limitations remain unaddressed. First, most current studies rely on linearized or semi-nonlinear models, failing to fully exploit the nonlinear dynamics of 6-DOF constructed using the Euler-Lagrange method, which may lead to discrepancies when applied in real operating conditions. Second, performance evaluations are often conducted under ideal conditions or with low noise levels, not adequately reflecting the actual operational environment, which is characterized by complex disturbances and uncertainties. Third, there is a lack of a standardized, comprehensive quantitative assessment framework, as many works provide only qualitative analysis or use incomplete evaluation metrics, often overlooking important indicators such as rise time, settling time, percentage overshoot, steady-state error, MSE, and RMSE. Finally, the integration of intelligent control methods with formation control problems remains limited, as fuzzy PID methods have primarily been developed for single UAVs. At the same time, their application to multi-UAV systems with geometric constraints has not been fully explored. These gaps highlight the urgent need for a control framework that integrates a comprehensive nonlinear model, adapts to disturbances, and provides a thorough quantitative performance evaluation method for UAV formation control problems.

This paper proposes a triangular formation control method based on a leader-follower structure for quadcopter UAVs, utilizing a Mamdani fuzzy PID controller on a fully nonlinear 6-DOF dynamic model. The proposed method integrates a fuzzy inference mechanism to adjust PID parameters in real time, thereby enhancing adaptability to nonlinearities and external disturbances. At the same time, an equilateral triangular formation structure is established to ensure geometric stability and coordination efficiency in the three-dimensional space. To evaluate performance, the study develops a multi-criteria quantitative assessment framework that includes both transient and steady-state metrics and extends to error measures such as MSE and RMSE under both noisy and noise-free conditions. Simulation results in the MATLAB/Simulink environment demonstrate that the proposed method significantly improves overshoot, steady-state error, and disturbance resistance compared to traditional PID controllers.

The main contributions of the research include: (i) Developing a comprehensive nonlinear 6-DOF dynamic model for multi-UAV systems based on the Euler-Lagrange equations; (ii) designing an adaptive Mamdani fuzzy PID controller for the leader-follower formation control problem; (iii) constructing a triangular formation with clear geometric constraints in 3D space; (iv) proposing a multi-criteria performance evaluation framework, including both time and energy error metrics (MSE, RMSE); and (v) conducting a comprehensive assessment under external disturbance conditions, demonstrating robustness and superiority over classical PID.

The paper is organized into five sections: Section 1, introduction; Section 2, presentation of the kinematic model of the quadcopter UAV; Section 3, description of the controller design and formation strategy; Section 4, presentation of simulation results and comparative analysis; and finally, Section 5, conclusions and future research directions.

2. Dynamic model of quadcopter UAV

This work considers a multi-UAV system composed of quadcopter agents, each driven by four rotor motors. Two pairs of symmetrically arranged counter-rotating rotors generate lift and provide complete three-dimensional motion control. Figure 1 depicts the general quadcopter structure.

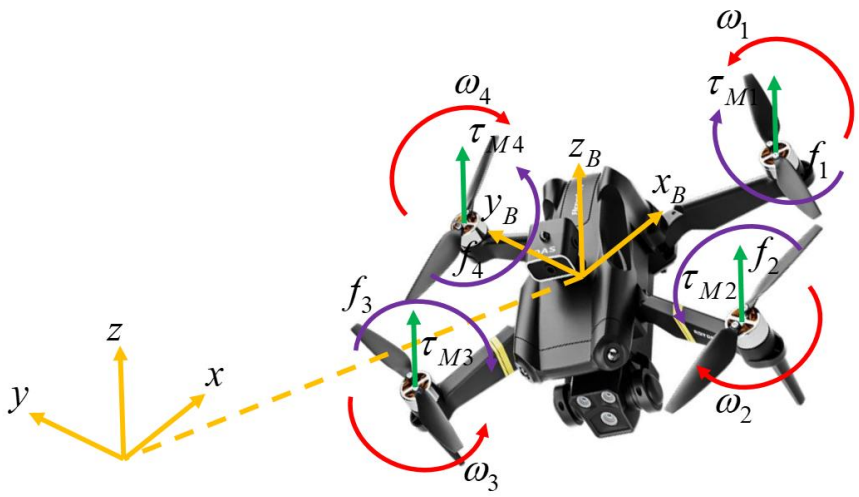

Figure 1. Structure of quadcopter UAVs in three-dimensional space.

The control system of quadcopter UAVs operates in six degrees of freedom (6-DOF), including three translational movements along the coordinate axes (x, y, z) and three rotational movements around the principal axes corresponding to the Euler angles: roll (φ), pitch (θ), and yaw (ψ). The author establishes the dynamic model of the quadcopter UAV using the Euler-Lagrange equations to capture the interactions among the forces and moments acting on the system. The four rotors generate lift collectively through their combined thrust. By varying the relative rotational speeds of the rotors, the controller regulates the rotational moments and governs the angular states. The system input control variables are constructed and presented as follows [4,5,10,11]:

$$\begin{aligned} F &= U_1 = k(\omega_1^2 + \omega_2^2 + \omega_3^2 + \omega_4^2) \\ \tau_\phi &= U_2 = l\ k\ (\omega_4^2 - \omega_2^2) \\ \tau_\theta &= U_3 = l\ k\ (\omega_3^2 - \omega_1^2) \\ \tau_\psi &= U_4 = b(\omega_1^2 - \omega_2^2 + \omega_3^2 - \omega_4^2) \end{aligned} \tag{1}$$

Where $\omega_\delta = \omega_1 - \omega_2 + \omega_3 - \omega_4$ denotes the total angular velocity of the four propellers, and F represents the collective thrust force generated along the body-fixed z-axis. The parameter k is the aerodynamic lift coefficient, b is the rotor drag (torque) coefficient, and l denotes the distance from the quadcopter's center of mass to each propeller. The control input U_1 corresponds to the total thrust produced by all rotors. At the same time, U_2, U_3, and U_4 represent the control torques about the roll (x-axis), pitch (y-axis), and yaw (z-axis), respectively, aligned with the quadcopter's principal inertia axes. This paper presents a complete set of translational and rotational kinematic equations for the UAV, formulated from a nonlinear 6-DOF Euler–Lagrange model and augmented with aerodynamic damping and external disturbance terms represented as generalized non-conservative forces [4,5,10,11].

$$\ddot{x} = \frac{F}{m}(\cos\psi \sin\theta \cos\phi + \sin\psi \sin\phi) - \frac{A_x \dot{x}}{m}$$
$$\ddot{y} = \frac{F}{m}(\sin\psi \sin\theta \cos\phi - \cos\psi \sin\phi) - \frac{A_y \dot{y}}{m}$$
$$\ddot{z} = \frac{F}{m}(\cos\phi \cos\theta) - g - \frac{A_z \dot{z}}{m}$$
$$\ddot{\phi} = \left(\frac{I_{yy} - I_{zz}}{I_{xx}}\right)\dot{\theta}\dot{\psi} - \left(\frac{I_M \omega_\delta}{I_{xx}}\right)\dot{\theta} + \left(\frac{\tau_\phi}{I_{xx}}\right) - \frac{A_\phi \dot{\phi}}{I_{xx}} \quad (2)$$
$$\ddot{\theta} = \left(\frac{I_{zz} - I_{xx}}{I_{yy}}\right)\dot{\psi}\dot{\phi} + \left(\frac{I_M \omega_\delta}{I_{yy}}\right)\dot{\phi} + \left(\frac{\tau_\theta}{I_{yy}}\right) - \frac{A_\theta \dot{\theta}}{I_{yy}}$$
$$\ddot{\psi} = \left(\frac{I_{xx} - I_{yy}}{I_{zz}}\right)\dot{\theta}\dot{\phi} + \left(\frac{\tau_\psi}{I_{zz}}\right) - \frac{A_\psi \dot{\psi}}{I_{zz}}$$

Here, ϕ, θ, ψ represent the roll, pitch, and yaw angles of the UAV, with their first and second time derivatives corresponding to angular velocities ($\dot{\phi}, \dot{\theta}, \dot{\psi}$) and angular accelerations ($\ddot{\phi}, \ddot{\theta}, \ddot{\psi}$), respectively. m is the quadcopter mass, I_M is the rotor inertia, and I_{xx}, I_{yy}, I_{zz} are the principal body inertias along the x-, y-, and z-axes. The coefficients A_x, A_y, A_z characterize the translational aerodynamic drag along the inertial frame axes, whereas A_ϕ, A_θ and A_ψ model the external disturbance moments influencing the roll, pitch, and yaw dynamics.

3. Proposed nonlinear control design and formation strategy

This paper proposes a cascade fuzzy PID control framework to ensure accurate trajectory tracking and stable formation maintenance of the nonlinear 6-DOF quadrotor UAV system. This architecture includes a position control loop (outer loop) and an attitude control loop (inner loop). Figure 2 presents the overall structure using the fuzzy PID controller for the quadcopter UAV. The outer loop adjusts the translational motion along the x-, y-, and z-axes. The position error is defined as follows:

$$e_x = x_d - x, e_y = y_d - y, e_z = z_d - z \quad (3)$$

Where x_d, y_d, z_d are the desired trajectory coordinates.

Since the roll angle (ϕ) and pitch angle (θ) indirectly govern horizontal motion, the position controller generates the desired attitude reference values:

$$\phi_d = f_x(e_x, \dot{e}_x), \theta_d = f_y(e_y, \dot{e}_y) \quad (4)$$

The independent fuzzy PID controllers directly regulate the altitude z and the azimuth angle ψ. The inner loop ensures rapid tracking of the desired values of ϕ_d, θ_d, and ψ_d. This cascade structure helps to separate the translational dynamics (slow) from the rotational dynamics (fast), thereby improving the stability and disturbance rejection of the closed-loop system.

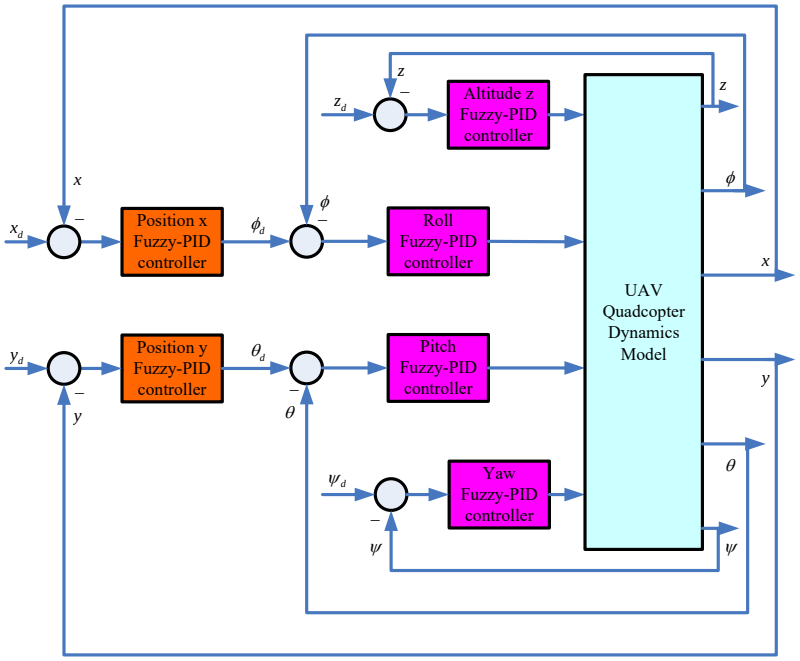

Figure 2. Overall control architecture of the fuzzy PID based quadcopter system.

3.1. Classical PID control law

Figure 3 illustrates the PID controller structure for each control channel, while Eq (5) defines the nominal PID control law.

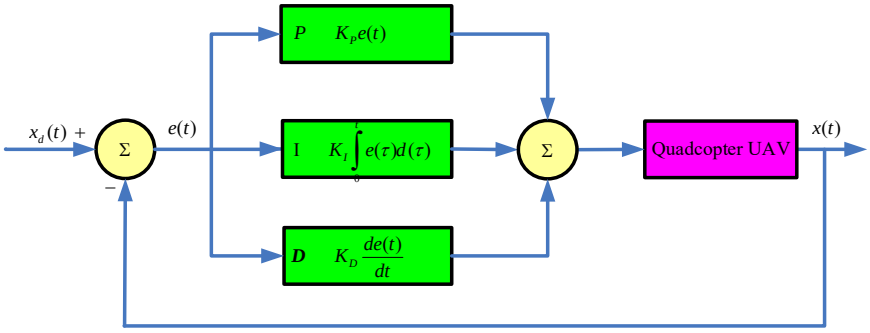

Figure 3. PID control structure for each control channel.

$$e(t) = x_d(t) - x(t)$$
$$u(t) = K_P e(t) + K_I \int_0^t e(\tau)d\tau + K_D \frac{de(t)}{dt} \tag{5}$$

In this formulation, the control input $u(t)$ is designed to optimize the system performance. The tracking error is defined as $e(t) = x_d(t) - x(t)$, where $x_d(t)$ denotes the reference trajectory, and $x(t)$ represents the system state. The classical PID controller is used as the basic control structure,

where the control signal is determined by the error, its integral, and its derivative, with fixed coefficients K_P, K_I, and K_D. This structure enables the development of a nominal control law for comparison with the proposed fuzzy PID controller. However, in 6-DOF nonlinear UAV systems, fixed PID coefficients often do not ensure optimal performance when parameter uncertainty, external disturbances, and wind noise are present. Therefore, the adaptive adjustment mechanism based on Mamdani fuzzy inference is presented separately in Section 3.2.

3.2. Design of the fuzzy PID controller

In high-order nonlinear dynamic systems such as the 6-DOF quadrotor UAV, using a PID controller with fixed coefficients often does not ensure optimal performance across the entire operating range. Changes in aerodynamic parameters, wind disturbances, payload, and interactions between axes can degrade control quality, leading to overshoot, prolonged settling times, or the emergence of residual oscillations. To overcome this limitation, an online adaptive mechanism based on a Mamdani fuzzy inference system is employed to tune the PID coefficients. This fuzzy inference system with two inputs allows for mapping the control output equivalent to the fuzzy PID controller presented in Figure 4.

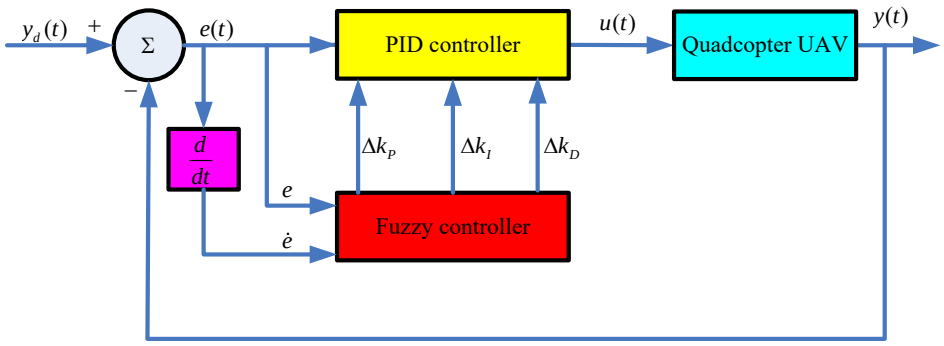

Figure 4. Mamdani fuzzy PID controller architecture for the quadrotor UAV.

The Mamdani fuzzy inference system is used to adapt the PID coefficients. The fuzzy controller receives two inputs, the error $e(t)$ and the derivative of the error $\dot{e}(t)$, and generates three normalized outputs $K_P^{'}, K_D^{'}$, and α. These outputs are subsequently utilized to update the effective parameters of the PID control law. Each variable is fuzzified using five membership functions, corresponding to the linguistic labels: NL (negative large), NS (negative small), Z (zero), PS (positive small), and PL (positive large). The membership functions are evenly distributed with centers at $-2,-1,0,1,2$, ensuring complete coverage of the variable's defined range and maintaining appropriate overlap between adjacent fuzzy sets. There are several methods for tuning the parameters of a PID controller, such as objective function–based tuning and direct tuning. Still, the simplest and most applicable method is the fuzzy tuning method by Zhao, Tomizuka, and Isaka, assuming that the parameters are constrained [35].

$$K_P \in \left[K_P^{\min}, K_P^{\max}\right], K_D \in \left[K_D^{\min}, K_D^{\max}\right] \tag{6}$$

Zhao, Tomizuka, and Isaka standardized those parameters as follows [28]:

$$K_P^{'} = \frac{K_P - K_P^{\min}}{K_P^{\max} - K_P^{\min}}, K_D^{'} = \frac{K_D - K_D^{\min}}{K_D^{\max} - K_D^{\min}} \tag{7}$$

where α is the fuzzy adjustment coefficient defined as $\alpha = \frac{K_I K_D}{K_P^2}$, representing the normalized relationship among the PID gains K_I, K_P, K_D. Based on this relationship, the integral gain is expressed as [35,36]:

$$K_I = \frac{\alpha K_P^2}{K_D} \tag{8}$$

The control coefficients are defined as follows [35,36]:

$$\begin{cases} K_P = (K_P^{\max} - K_P^{\min}) K_P^{'} + K_P^{\min} \\ K_D = (K_D^{\max} - K_D^{\min}) K_D^{'} + K_D^{\min} \\ K_I = \frac{\alpha K_P^2}{K_D} \end{cases} \tag{9}$$

The fuzzy system uses IF-THEN rules with a total of 5 × 5 = 25 fuzzy control rules constructed based on the principle of bias-centered reasoning. The controller reduces the control gain when both the tracking error and its derivative become significant, thereby mitigating overshoot and oscillatory behavior.

Table 1. Fuzzy rule base of the fuzzy PID controller.

$e(t)$ \ $\dot{e}(t)$	**NL**	**NS**	**Z**	**PS**	**PL**
NL	NL	NL	NS	Z	PS
NS	NL	NS	Z	PS	PL
Z	NS	Z	Z	Z	PS
PS	Z	PS	Z	PS	PL
PL	PS	PL	PS	PL	PL

The combination of fuzzy rules, fuzzy sets, and the Mamdani inference system establishes a nonlinear mapping from the input space to the output control signal, where the two input variables are the position error and its derivative, processed by a rule set of 25 IF-THEN rules. This structure allows adaptive adjustment of the equivalent PID coefficients based on the system's operational state, rather than using fixed parameters. When the error is large or the rate of change is high, the fuzzy inference mechanism reduces the effective gain to limit oscillations and overshoot during the transient phase; conversely, as the system approaches the steady-state, the control coefficients are fine tuned to increase sensitivity to small errors, thereby improving accuracy and reducing steady-state error. This mechanism can be viewed as a form of nonlinear gain scheduling, in which

the control parameters are not fixed but continuously adapt to the system's state. As a result, the fuzzy PID controller achieves an effective balance between transient and steady-state performance, particularly in nonlinear 6-DOF dynamic systems affected by disturbances and parameter uncertainties, which explains the significant improvement in steady-state error and the MSE and RMSE metrics compared to the classical PID controller.

After optimizing the control parameters, the fuzzy PID controller is implemented in the quadcopter system's control model to enhance trajectory stability and improve real-time control accuracy. The effectiveness of the control is evaluated through numerical simulations in the MATLAB/Simulink environment, focusing on analyzing the system's kinematic response under ideal conditions, unaffected by noise or environmental variations. The simulation results show that the system can maintain the desired trajectory with minimal error, demonstrating the effectiveness of the control algorithm. This integrated control model helps the UAV achieve high performance in stability and trajectory tracking under standard operating conditions.

3.3. Triangular formation structure

To ensure that the UAVs maintain a stable triangular formation in the three-dimensional space, the author proposes a leader-follower formation control strategy. This method combines trajectory tracking control for the lead UAV with relative-position control for the following UAVs. The proposed framework establishes an equilateral triangle in the xy plane, with UAV 1 as the leader and UAV 2 and UAV 3 as follower agents. Each follower will track a predetermined relative position ΔP_i with respect to the leader, thereby maintaining the geometric formation throughout the movement. The equation describing the desired position of each UAV is as follows:

$$P_i^{ref}(t) = P_L(t) + R_L(t)\Delta P_i, i = 1,2,3 \tag{10}$$

Where $P_i^{ref}(t)$ is the reference position vector of the i-th UAV at time t, $P_L(t)$ is the position vector of the leader UAV at time t, $R_L(t)$ is the rotation matrix associated with the leader attitude, and ΔP_i is the static geometric offset vector, defining the desired relative position of the i-th UAV with respect to the leader UAV in the formation. The use of rotation matrices in formation representation is a standard approach in multi-agent formation control problems, allowing for the preservation of geometric structure in the three-dimensional space [37].

The rotation matrix $R_L(t)$ is constructed based on the Euler angles (ϕ_L, θ_L, ψ_L) as follows [38]:

$$R_L(t) = R_z(\psi_L)R_y(\theta_L)R_x(\phi_L) \tag{11}$$

Where $R_z(\psi_L), R_y(\theta_L), R_x(\phi_L)$ are the standard rotation matrices around the z-, y-, and x-axes, respectively. This representation is widely used in recent studies on UAV formation control and multi-agent systems in the SE(3) space, particularly in attitude control and maintaining formation structure [37].

In this study, since the motion primarily occurs in the horizontal plane, the rotation matrix is approximated as follows:

$$R_L(t) \approx R_z(\psi_L) \tag{12}$$

This ensures that the formation rotates synchronously with the leading UAV during the

maneuvering process. This simplification is also commonly applied in UAV systems operating in real-world environments to reduce computational complexity while still maintaining the accuracy of the formation structure [38].

The above equation defines the centralized control principle adopted in the leader-follower UAV formation framework. The control architecture drives the leader UAV to track a predefined global reference trajectory, while the follower UAVs maintain prescribed relative positions with respect to the leader using predetermined geometric offset vectors ΔP_i.

This structure simplifies the overall formation control problem and reduces communication bandwidth and latency requirements, since the system requires only one-way information transmission from the leader to the followers.

The geometric offset vectors are defined as follows:

$$\Delta P_1 = \begin{bmatrix} 0 \\ 0 \\ 0 \end{bmatrix} (Leader),\ \Delta P_2 = \begin{bmatrix} d \\ 0 \\ 0 \end{bmatrix} (Follower1), \Delta P_3 = \begin{bmatrix} \frac{d}{2} \\ -\frac{\sqrt{3}}{2} d \\ 0 \end{bmatrix} (Follower2) \tag{13}$$

The parameter d > 0 is the desired distance between UAVs and simultaneously determines the lengths of the sides of the equilateral triangle formation. The value of this parameter directly influences the geometric scale of the formation and significantly impacts collision avoidance capabilities, communication range, and the sensor coverage area of the UAV system [39]. In the formation coordinate system, ΔP_1 represents the position of the leading UAV, serving as a reference point. At the same time, ΔP_2 and ΔP_3 describe the relative positions of the two following UAVs, arranged so that together with the leading UAV, they form an equilateral triangle in the three-dimensional space.

This structure forms an equilateral triangle in the xy plane, with each side measuring 1 m, ensuring that the follower UAVs always maintain the corresponding distance and orientation relative to the leader UAV, regardless of their absolute position in space. This arrangement is a crucial basis for designing centralized or decentralized control strategies to ensure stability and maintain the UAV formation in complex flight scenarios. Figure 5 presents the triangular formation leader-follower strategy.

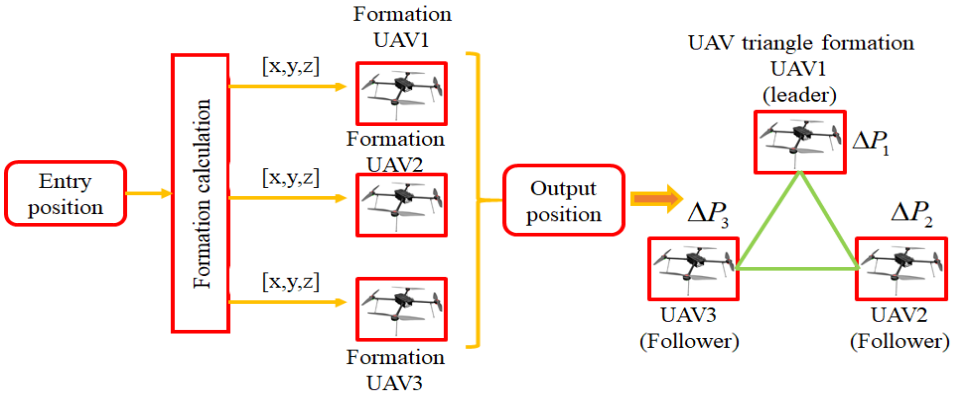

Figure 5. Leader-follower triangular formation geometry of the three UAV system.

In UAV formation control, maintaining formation using fixed geometric displacement vectors offers numerous advantages in both computation and practical implementation. Specifically, controlling only the lead UAV along a reference trajectory significantly reduces the computational complexity of the entire system, as the following UAVs only need to maintain a predetermined relative position to the leader. The proposed strategy simplifies the control algorithm implemented on each UAV and reduces the real-time computational burden required for onboard processing. Furthermore, this method significantly reduces communication latency because it does not require each UAV to continuously exchange data with all other UAVs, unlike distributed or consensus-based control strategies. Due to its high centralization, the UAV system operates as a unified entity while still maintaining a simple control structure, making it particularly suitable in cases with limited computational capacity or communication bandwidth. A significant advantage of the proposed centralized strategy lies in its reduced onboard computational burden. In contrast, distributed control approaches require each UAV to process information received from neighboring agents and continuously update its local state estimates and control inputs in real time, thereby increasing communication overhead and computational complexity.

4. Simulation results

This study utilizes MATLAB to simulate UAV formations due to its strong control system analysis tools and flexibility in modeling nonlinear dynamics. MATLAB not only provides tools for accurately simulating the complex dynamics of quadcopters but also facilitates the testing, tuning, and optimization of control strategies in a simulated environment. Through this process, the stability and performance of the controller can be comprehensively evaluated before experimental deployment, thereby helping minimize errors and costs during actual testing. This study defines the specific technical parameters of the UAV model as summarized in Table 2.

Table 2. Physical parameters of the quadcopter UAV.

Parameter	Symbol	Value
Quad. mass	m	0.468 kg
Arm length	l	0.225 m
Gravity	g	9.81 m/s^2
Inertia moment of the rotor	I_M	3.357e-5 $kg.m^2$
Thrust factor of rotor	k	2.980e-6 $N.s^2$
Drag coefficient	b	1.140e-7 $N.m.s^2$
Inertial constants	I_{xx}, I_{yy}	4.856e-3 $kg.m^2$
	I_{zz}	8.801e-3 $kg.m^2$
Aerodynamic friction coefficients	A_x, A_y, A_z	0.25
Translational drag coefficients	A_ϕ, A_θ, A_ψ	

Figures 6 and 7 illustrate the position response of the UAV system when maintaining a triangular formation in three-dimensional space and along each coordinate axis. Figure 6 shows the 3D trajectories of the UAVs along the x, y, and z components, visually demonstrating the ability to maintain the triangular formation in three dimensions. This result indicates that the UAVs closely follow the desired trajectory with minimal deviation, smooth motion, and no significant oscillations,

demonstrating that the controller maintains trajectory stability and preserves the relative distances within the formation. Meanwhile, Figure 7 presents the responses along each axis (x, y, z) as time signals, enabling quantitative assessment of settling time, overshoot, and steady-state error. The response curves converge quickly to the reference values, exhibit small transient oscillations, and show no signs of instability, indicating that the system can adapt well to the requirements of formation movement. The results also show that the controller not only ensures trajectory accuracy along each axis but also maintains the geometric integrity of the triangular formation in the three-dimensional space, which is particularly important for UAV swarm applications that require tight coordination and high reliability.

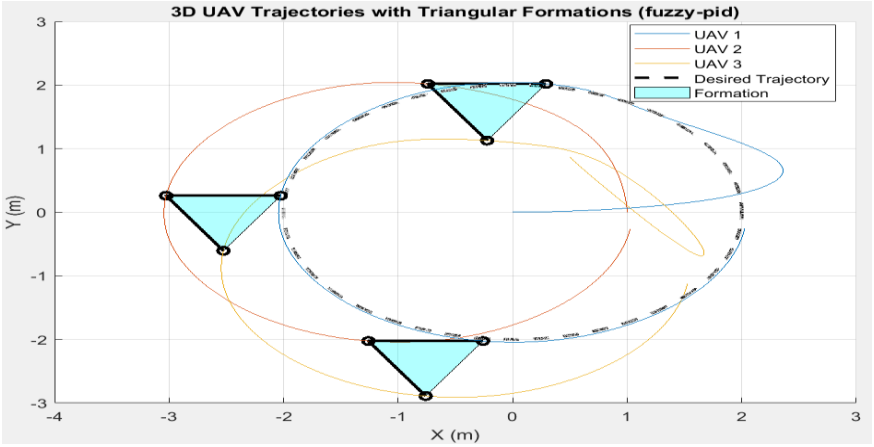

Figure 6. 3D position response x, y, z with triangular formation.

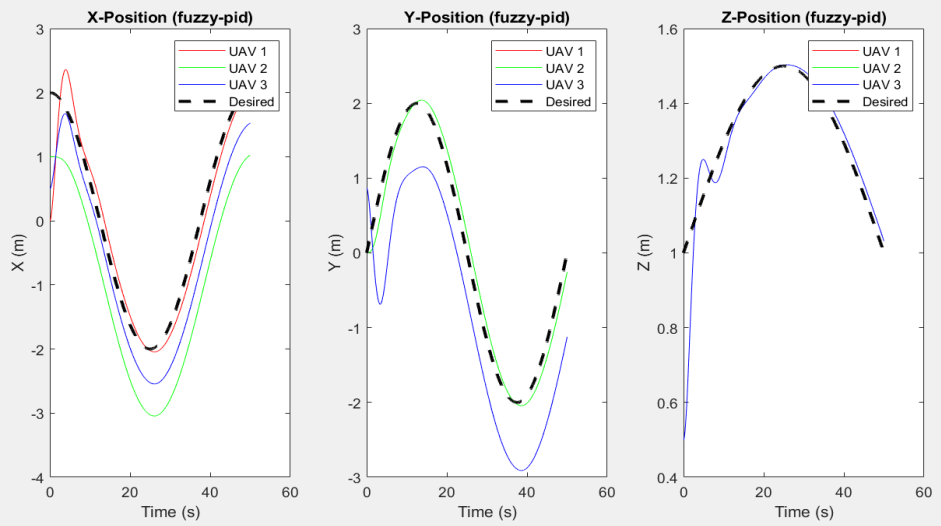

Figure 7. Position response x, y, z with triangular formation.

Figure 8 and Table 3 provide a visual and quantitative representation of the UAV controller's performance in the triangular formation. Figure 8 shows the position tracking error of UAV1 over time, directly reflecting the control system's ability to maintain the desired trajectory. The error curve shows an initially relatively large oscillation amplitude during the transient phase, which then gradually decreases and converges to near zero, indicating that the system achieves a stable state

after a specific settling time. This result aligns with the quality metrics presented in Table 3, where the rise time is 12.93 s, and the settling time is approximately 50.00 s, indicating that the system has a relatively slow response but ensures stable convergence. The overshoot of 50.30% reflects the dynamic characteristics, which still oscillate significantly during the transient phase; however, the steady-state error is minimal (0.0315 m), indicating high accuracy upon reaching a stable state. These results further affirm the controller's effectiveness in maintaining a stable UAV position and in adequately meeting the technical criteria for navigation and coordination of UAV formations.

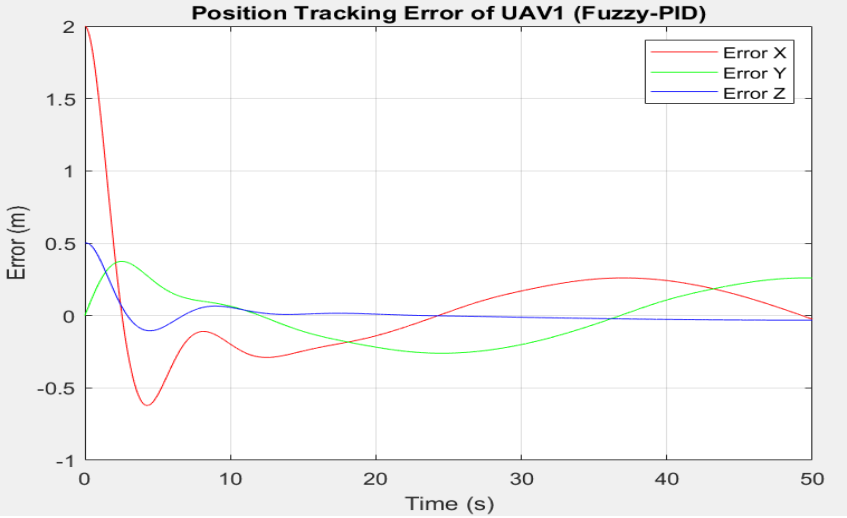

Figure 8. Position tracking error of UAV1 in the triangular formation.

Table 3. Quality indexes of UAV1 in the triangular formation at altitude Z (noise-free conditions).

Formation / Quality index	Triangular formation
Rise time (s)	12.93
Steady time (s)	50.00
Overshoot (%)	50.30
Steady-state error (m)	0.0315

The responses in Figures 9 and 10 evaluate the UAV system's robustness and disturbance rejection capability while maintaining a triangular formation under external disturbances. Figure 9 presents the 3D trajectories of the UAVs along the x, y, and z components in the presence of noise, showing that the formation's geometric structure is still preserved in 3D. Although temporary deviations occur due to disturbances, the trajectories quickly correct and return to the desired path, demonstrating that the controller can filter out noise and maintain relatively good trajectory stability. Additionally, Figure 10 shows the response along each coordinate axis over time under the same noisy conditions, allowing for precise observation of the kinematic characteristics in each direction of motion. The position signals exhibit larger transient oscillations than in the noise-free case; however, they still converge to the reference values after a settling time without any signs of instability. The results demonstrate that the system maintains stable formation geometry and trajectory tracking performance under external disturbances, thereby confirming its robustness to noise and its ability to preserve formation integrity.

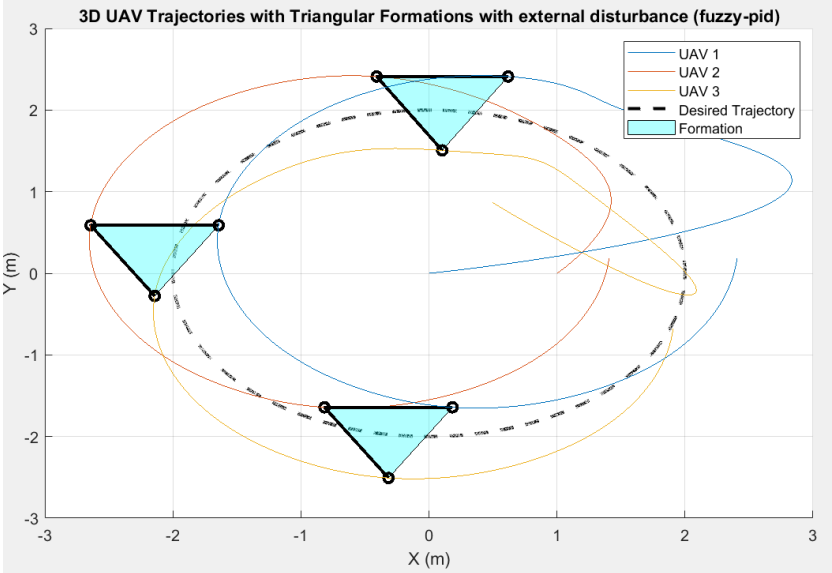

Figure 9. 3D position response x, y, z with triangular formation under external disturbance.

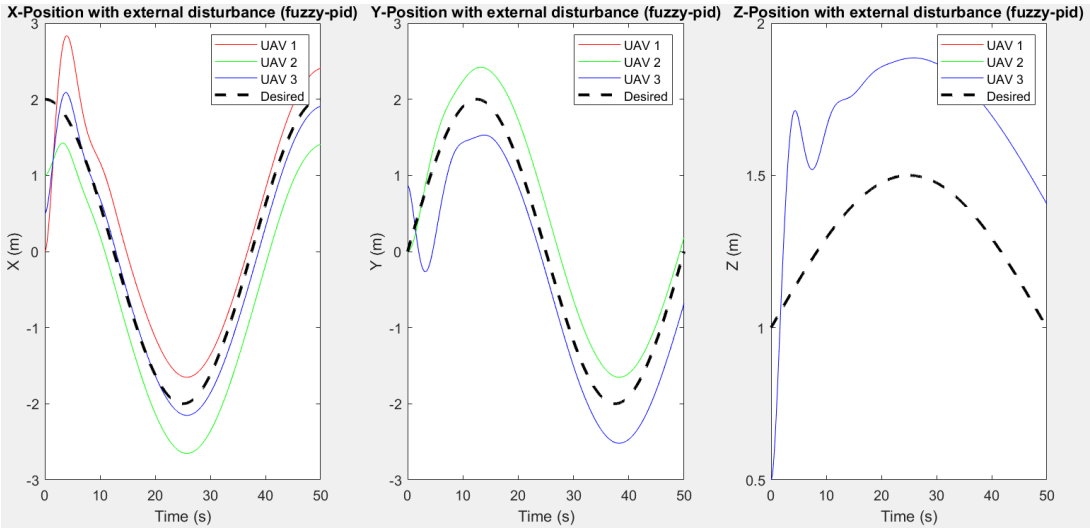

Figure 10. Position response x, y, z with triangular formation under external disturbance.

The results in Figure 11 and Table 4 comprehensively evaluate the trajectory tracking characteristics of UAV1 in the triangular formation when subjected to external disturbances along the altitude axis z. Figure 11 shows the position tracking error over time, indicating that the system experiences significant oscillations during the transient phase with considerable error amplitude immediately after being affected by noise. Although the response tends to converge to a stable state, the initial level of oscillation and the sustained deviation during the settling process indicate performance degradation relative to the noise-free case. The quantitative results in Table 4 support this observation, as the rise time decreases to 3.59 s, indicating a faster response to the disturbance signal; however, the overshoot increases significantly to 88.58%, demonstrating high transient oscillation and suboptimal adjustment capability under the influence of noise. The system exhibits a steady-state error of 0.4060 m, which is substantially higher than that observed under noise-free conditions, indicating a static deviation caused by environmental disturbances. Although the controller maintains stability and the settling time remains at 50.00 s, these results reveal limited

robustness under strong disturbance conditions. The results also show that the system retains the formation and overall stability. Still, improvements in noise filtering and overshoot reduction are needed by tuning control parameters or integrating robust control strategies to enhance response quality in real world environmental conditions.

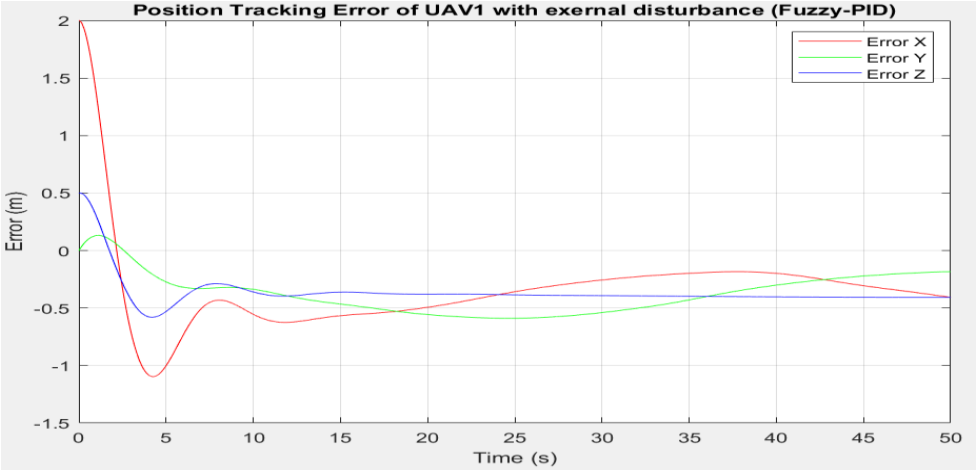

Figure 11. Position tracking error of UAV1 in the triangular formation under external disturbance.

Table 4. Quality indexes of UAV1 in the triangular formation under external disturbance at altitude Z.

Formation / Quality index	Triangular formation
Rise time (s)	3.59
Steady time (s)	50.00
Overshoot (%)	88.58
Steady-state error (m)	0.4060

In this study, the performance of the controllers is evaluated and compared through the quantitative metrics MSE and RMSE, aiming to provide a comprehensive analysis of the error characteristics of the system.

The mean squared error (MSE) metric is defined according to (14). This quantity reflects the average of the squared errors, thereby representing the average energy level of the error signal. Squaring the errors increases the influence of larger errors, making MSE sensitive to outliers. Therefore, the smaller the MSE value, the better the performance of the control system.

The mean squared error (MSE) is calculated as follows:

$$MSE = \frac{1}{T}\int_0^T e^2(t)dt;\ T - \text{calculated time period} \tag{14}$$

The root mean squared error (RMSE) metric is defined according to (15). RMSE represents the average magnitude of the error and has the same unit as the output variable, making it more convenient for interpretation and visual assessment. Essentially, RMSE provides information about the average deviation between the output signal of the controller and the desired setpoint value. Like MSE, RMSE is also sensitive to outliers because it depends on the square of the error.

The root mean squared error (RMSE) is calculated as follows:

$$RMSE = \sqrt{\frac{1}{T}\int_0^T e^2(t)dt};\ T - \text{calculated time period} \tag{15}$$

To comprehensively evaluate and compare the performance of traditional PID control and fuzzy PID control strategies in maintaining a triangular formation of the UAV system, the simulation results presented in Figures 12–15 demonstrate significant differences in dynamic response quality. Figure 12 shows the 3D trajectory response along the x, y, and z components, indicating that the fuzzy PID controller maintains a smoother trajectory, with fewer geometric deviations and better preservation of the formation structure compared to the classical PID. This difference becomes more pronounced when observing the individual responses along each axis in Figure 13 (x-axis), Figure 14 (y-axis), and Figure 15 (z-axis). Along the x- and y-axes, fuzzy PID exhibits lower transient oscillation amplitudes, shorter convergence times, and minor steady-state errors, reflecting better nonlinear adaptability to the system's kinematic variations. For the z-axis altitude, which is sensitive to noise and changes in lift, fuzzy PID shows a more stable response with significantly reduced overshoot compared to traditional PID. Scientifically, this can be explained by the fuzzy controller's flexible parameter adjustment mechanism, which allows updating the gain coefficients based on the error state and its rate of change, whereas classical PID uses fixed parameters. Overall, the results from Figures 12-15 demonstrate that fuzzy PID significantly improves trajectory tracking quality and the robustness of the UAV system in triangular formation, particularly under strong nonlinearities and complex dynamic interactions, thereby affirming the superiority of intelligent control methods over traditional linear control in UAV swarm applications.

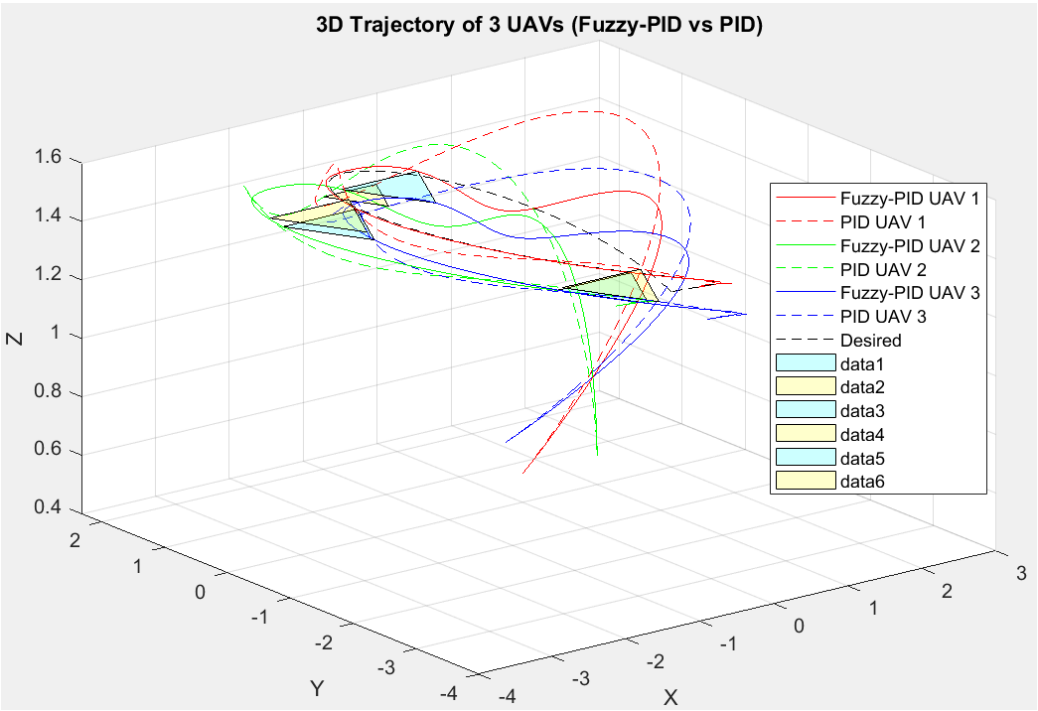

Figure 12. 3D position response x, y, z with triangular formation using fuzzy PID and PID controllers.

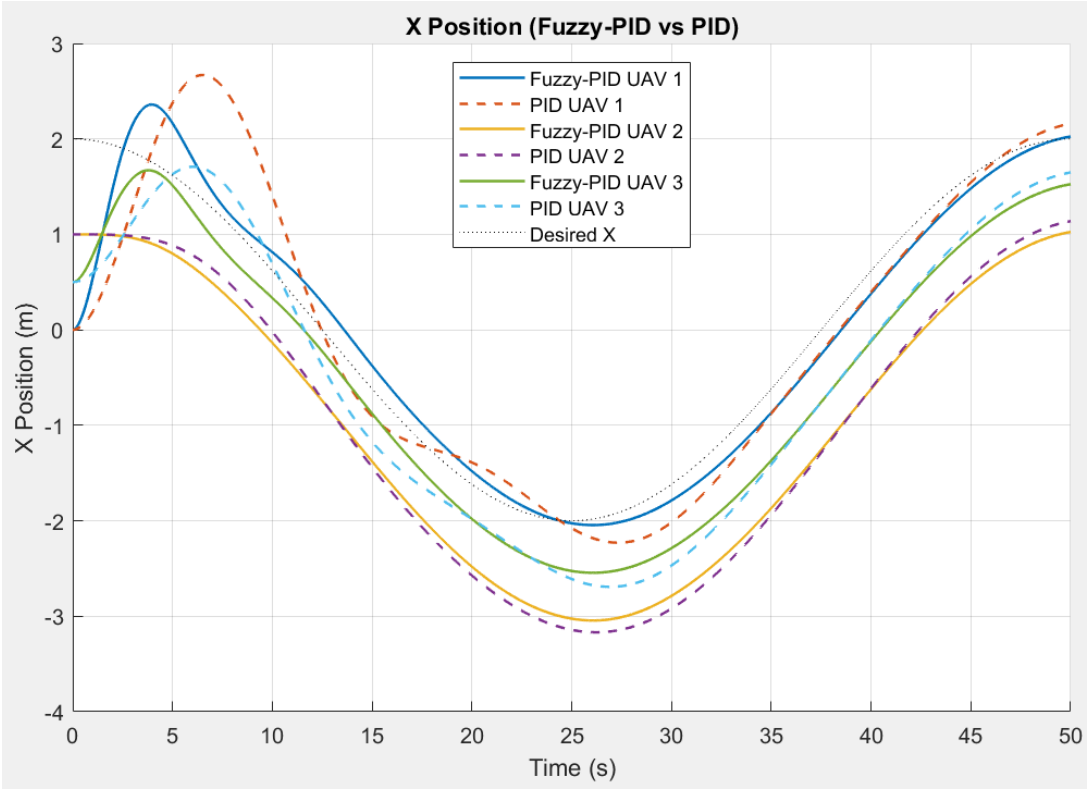

Figure 13. X position response with triangular formation using fuzzy PID and PID controllers.

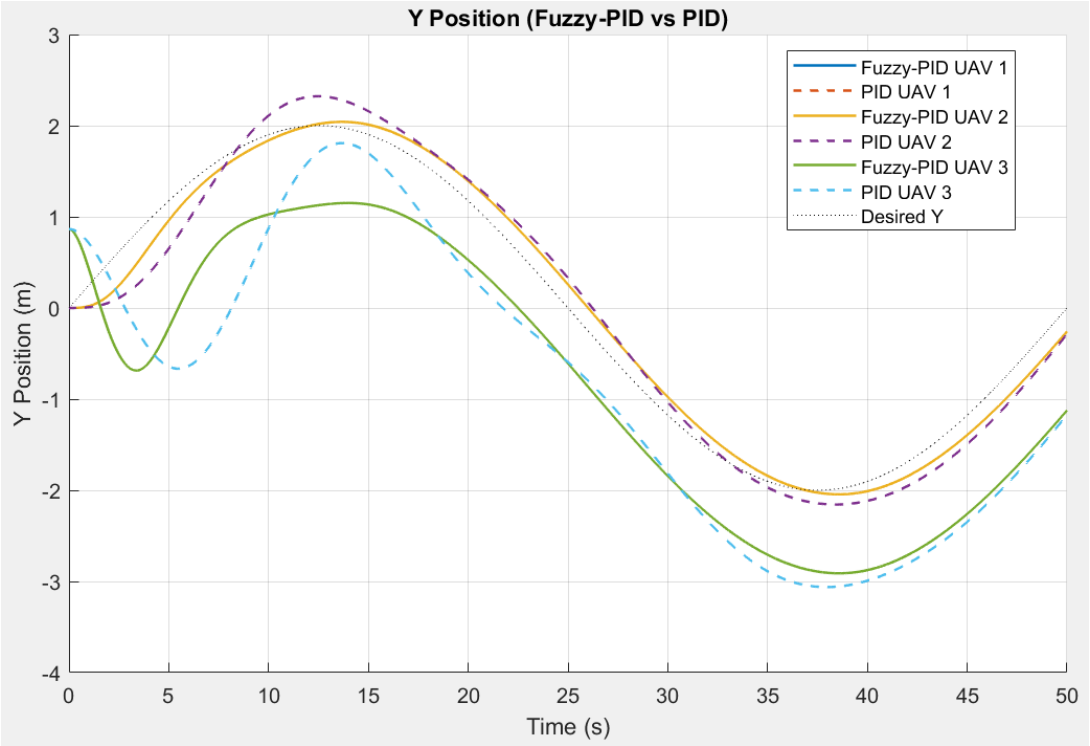

Figure 14. Y position response with triangular formation using fuzzy PID and PID controllers.

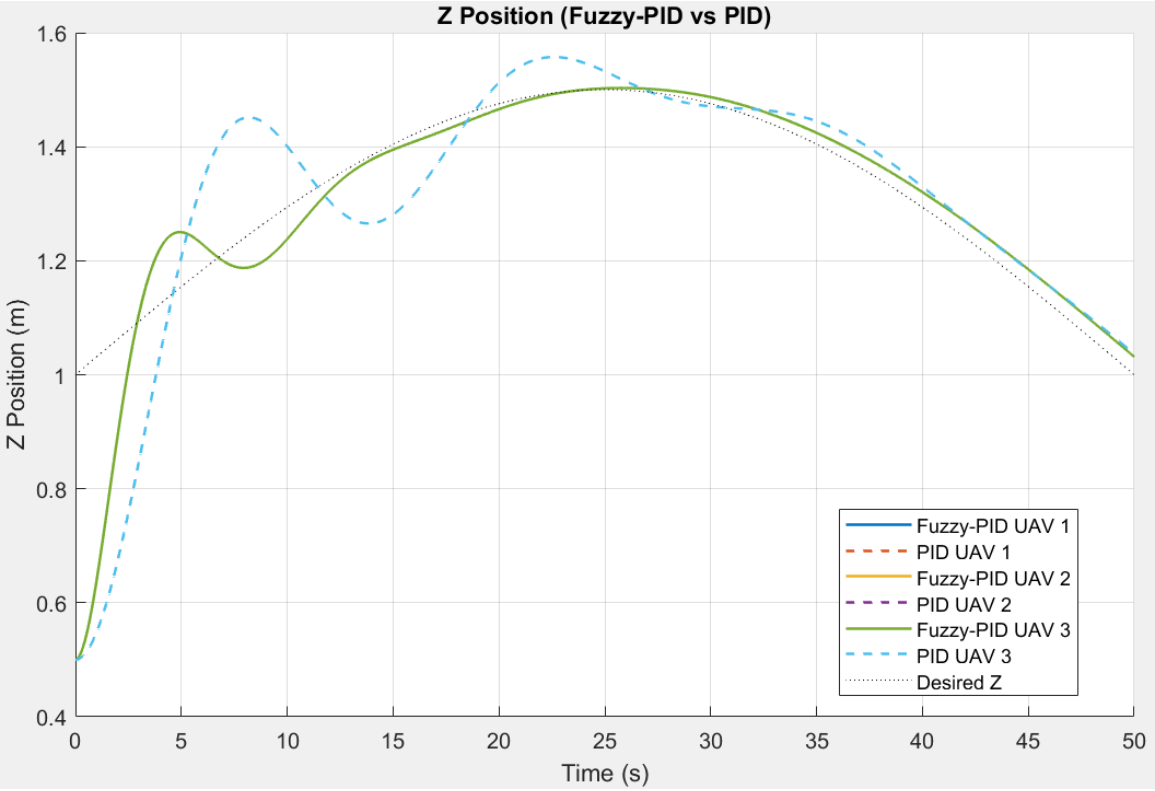

Figure 15. Z position response with triangular formation using fuzzy PID and PID controllers.

Table 5 presents the quantitative metrics used to compare the altitude control effectiveness (z-axis) between the fuzzy PID and traditional PID methods for a formation of three UAVs. The quality indicators include rise time, settling time, overshoot, and steady-state error, clearly reflecting the feedback capability and accuracy of each control strategy. Notably, fuzzy PID significantly reduces the rise time (2.03 s compared to 3.29 s), indicating a faster response to the input signal. Although both methods achieve similar settling times (approximately 50.01 s), fuzzy PID still shows an advantage with a lower overshoot (50.30% compared to 55.74%), demonstrating its ability to limit excessive oscillations during the transient phase. More importantly, the steady-state error for fuzzy PID is 0.0315 m, which is lower than that of PID (0.0365 m), proving higher accuracy in stabilizing the desired altitude. Thus, the quantitative results in Table 5 indicate that fuzzy PID not only improves response time but also enhances accuracy and regulation capability, thereby improving UAV control performance in a three-dimensional spatial formation.

Table 5. Evaluation of average quality control metrics for three UAVs in triangular formation at altitude Z between fuzzy PID and PID controllers (noise-free conditions).

Formation / Quality index	Triangular formation (fuzzy PID)	Triangular formation (PID)
Rise time (s)	2.03	3.29
Steady time (s)	50.01	50.01
Overshoot (%)	50.30	55.74
Steady-state error (m)	0.0315	0.0365

Table 6 presents quantitative comparisons between the PID controller and the fuzzy PID under noise-free conditions, using the MSE and RMSE metrics across the three axes x, y, and z. The results show that the fuzzy PID achieves superior performance across all axes, with both MSE and RMSE values significantly lower than those of the PID. Specifically, on axes x and y, the error decreases by approximately 17.98% and 24.7%, respectively, while on axis z, the improvement is even more pronounced, with MSE reduced by over 56.9%. The simulation and experimental results demonstrate that the fuzzy PID controller significantly enhances trajectory tracking accuracy and reduces system oscillations. Overall, the simultaneous reduction of both MSE and RMSE confirms the higher effectiveness and stability of the fuzzy PID controller compared to the traditional PID under ideal conditions.

Table 6. Quantitative comparison of control performance between PID and fuzzy PID controllers (noise-free conditions).

Quality index / Controller	MSE (PID)	MSE (fuzzy PID)	RMSE (PID)	RMSE (fuzzy PID)
X	0.609964	0.50030	0.7540	0.6525
Y	0.381490	0.287263	0.5171	0.4228
Z	0.016590	0.007147	0.1288	0.0845

To comprehensively assess the system's performance under disturbance environmental conditions, Figures 16-19 enable a comparative analysis of the performance of traditional PID controllers and fuzzy PID controllers when the UAV system maintains a triangular formation under disturbances. Figure 16 illustrates the 3D trajectories along the x, y, and z components in a noisy environment, showing that fuzzy PID maintains a more stable geometric structure of the formation, with smoother trajectories and minor spatial deviations than classical PID. This difference is more pronounced when analyzing each coordinate axis individually in Figure 17 (x-axis), Figure 18 (y-axis), and Figure 19 (z-axis). Along the horizontal x- and y-axes, traditional PID exhibits large transient oscillations and prolonged convergence times when subjected to noise. At the same time, fuzzy PID demonstrates lower oscillation amplitudes and faster recovery to stable states. Notably, on the z-axis, which is sensitive to variations in lift and aerodynamic disturbances, fuzzy PID shows higher robustness, with significantly reduced overshoot and maintained deviations. Overall, the results from Figures 16–19 demonstrate that under uncertain environmental conditions, fuzzy PID outperforms traditional PID in noise filtering, stability maintenance, and formation preservation, thereby affirming the effectiveness of intelligent control methods in UAV swarm applications operating in highly dynamic real-world environments.

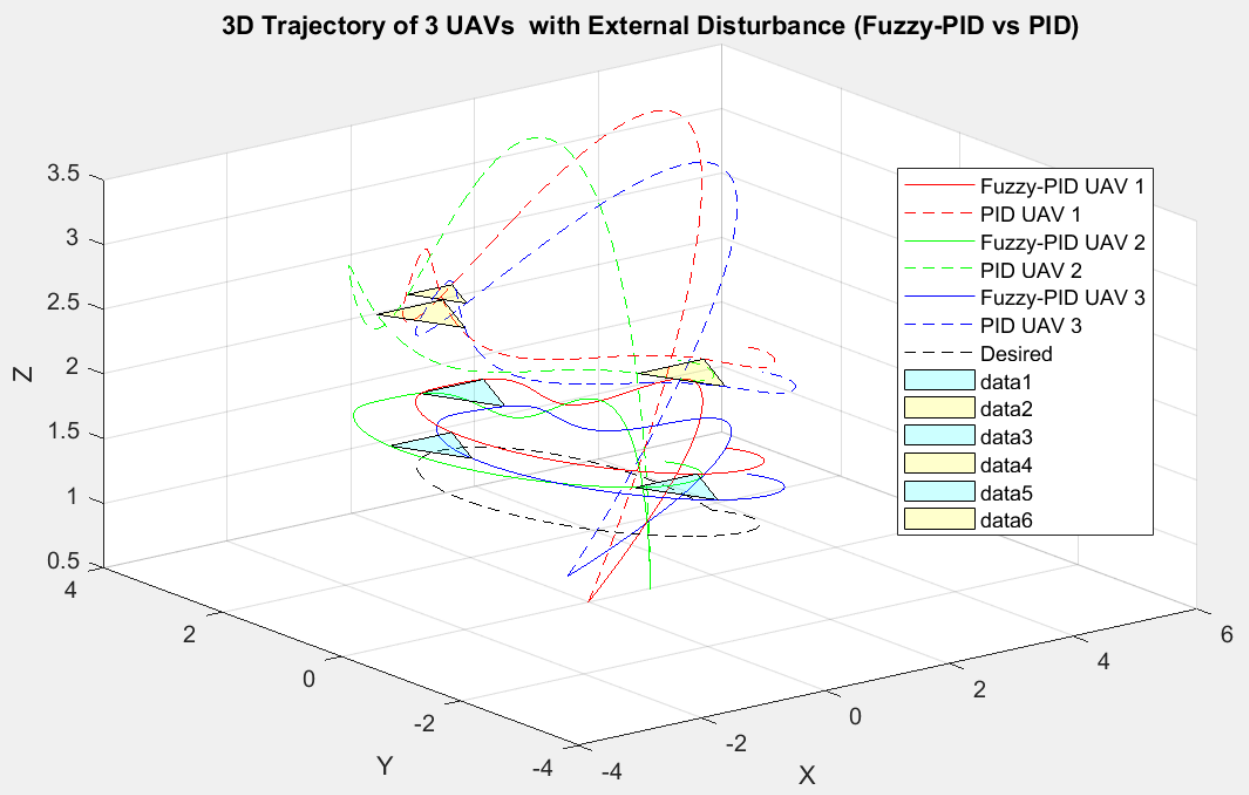

Figure 16. 3D position response x, y, z with triangular formation using fuzzy PID and PID controllers under external disturbance.

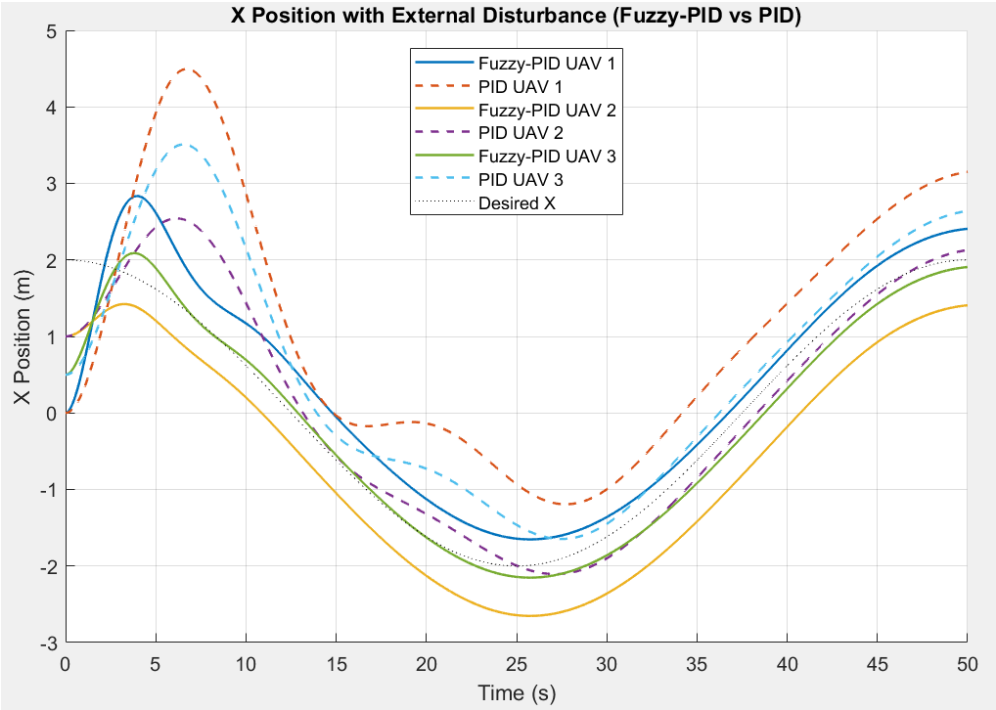

Figure 17. X position response with triangular formation using fuzzy PID and PID controllers under external disturbance.

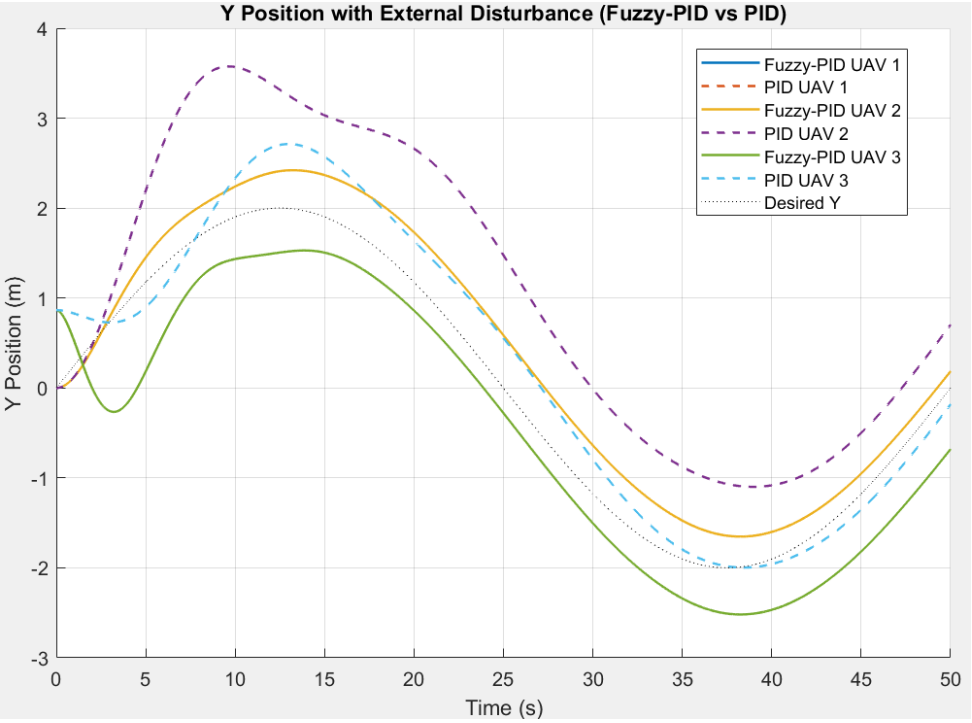

Figure 18. Y position response with triangular formation using fuzzy PID and PID controllers under external disturbance.

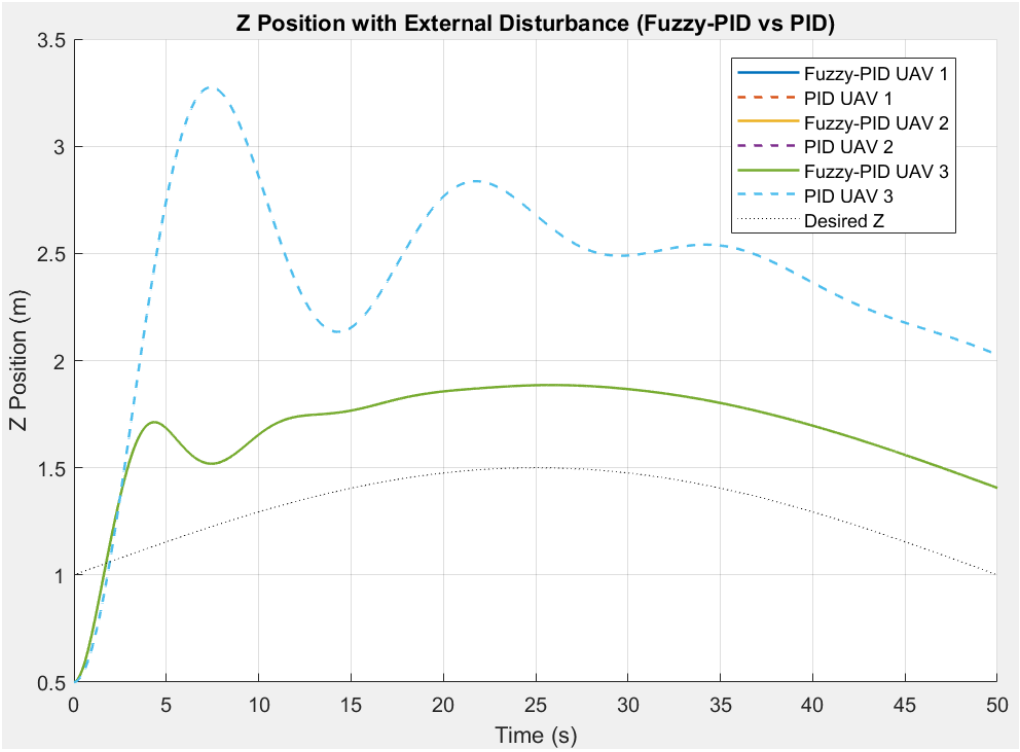

Figure 19. Z position response with triangular formation using fuzzy PID and PID controllers under external disturbance.

Table 7 quantitatively evaluates the average control performance of the three UAVs operating in a triangular formation under external disturbances applied along the z-axis. The table directly compares the performance of the PID and fuzzy PID control strategies. The results show that fuzzy PID achieves a rise time of 1.40 s, which is shorter than the 1.62 s for traditional PID, reflecting a quicker response to system fluctuations. Although the settling time for both methods is nearly equivalent (50.01 s), a significant difference is evident in the overshoot and steady-state error. Specifically, the overshoot for fuzzy PID is 88.58%, much lower than the 227.50% for PID, indicating that the fuzzy controller significantly reduces transient oscillations under noise conditions. At the same time, the steady-state error for fuzzy PID is 0.4060 m, considerably less than the 1.0272 m for PID, demonstrating higher stability and accuracy in the steady-state. Overall, Table 7 shows that fuzzy PID outperforms traditional PID in noise filtering, reducing transient oscillations, and enhancing trajectory tracking accuracy, thereby improving the effectiveness of maintaining the formation of the UAV system.

Table 7. Evaluation of average quality control metrics for three UAVs in triangular formation at altitude Z using fuzzy PID and PID controllers (external disturbance conditions).

Formation / Quality index	Triangular formation (fuzzy PID)	Triangular formation (PID)
Rise time (s)	1.40	1.62
Steady time (s)	50.01	50.01
Overshoot (%)	88.58	227.50
Steady-state error (m)	0.4060	1.0272

Table 8 presents a quantitative comparison of control performance between PID and fuzzy PID under conditions with external noise and wind disturbance, using MSE and RMSE metrics across the x-, y-, and z-axes. The results show that fuzzy PID significantly outperforms PID, with substantial reductions in error across all axes; specifically, the MSE decreases by approximately 72.5% (x-axis), 78.1% (y-axis), and 88.8% (z-axis). At the same time, RMSE decreases correspondingly, reflecting the ability to reduce oscillations and improve trajectory tracking accuracy. These results confirm that fuzzy PID has better noise resistance and maintains greater stability, making it more suitable for UAV systems operating in real-world noisy environments.

Table 8. Quantitative comparison of control performance using PID and fuzzy PID controllers (external disturbance conditions).

Quality index / Controller	MSE (PID)	MSE (fuzzy PID)	RMSE (PID)	RMSE (fuzzy PID)
X	0.932266	0.256639	0.8894	0.4859
Y	0.938519	0.205686	0.9004	0.4501
Z	1.364383	0.153018	1.1681	0.3912

Figures 20-23 present the position response of a trio of UAVs flying in a triangular formation in the three-dimensional space under the influence of external noise and wind disturbance, utilizing two controllers: PID and fuzzy PID. Figure 20 illustrates the 3D trajectory along the x-, y-, and z-axes,

showing that the fuzzy PID controller enables the UAVs to follow the desired trajectory more smoothly, with smaller deviations and less oscillation compared to PID. Figures 21-23 provide a detailed analysis for each axis: on the x- and y-axes, fuzzy PID demonstrates the ability to reduce oscillations and shorten settling time, whereas PID exhibits larger oscillations and a longer stabilization time. On the z-axis (Figure 23), the difference is even more pronounced, as fuzzy PID maintains a more stable altitude under the influence of wind disturbance, with significantly smaller deviations and less oscillation compared to PID. The results indicate that these images align with the quantitative analysis, confirming that fuzzy PID significantly enhances trajectory tracking performance, increases noise resistance, and ensures stability for UAV systems in real-world operating environments.

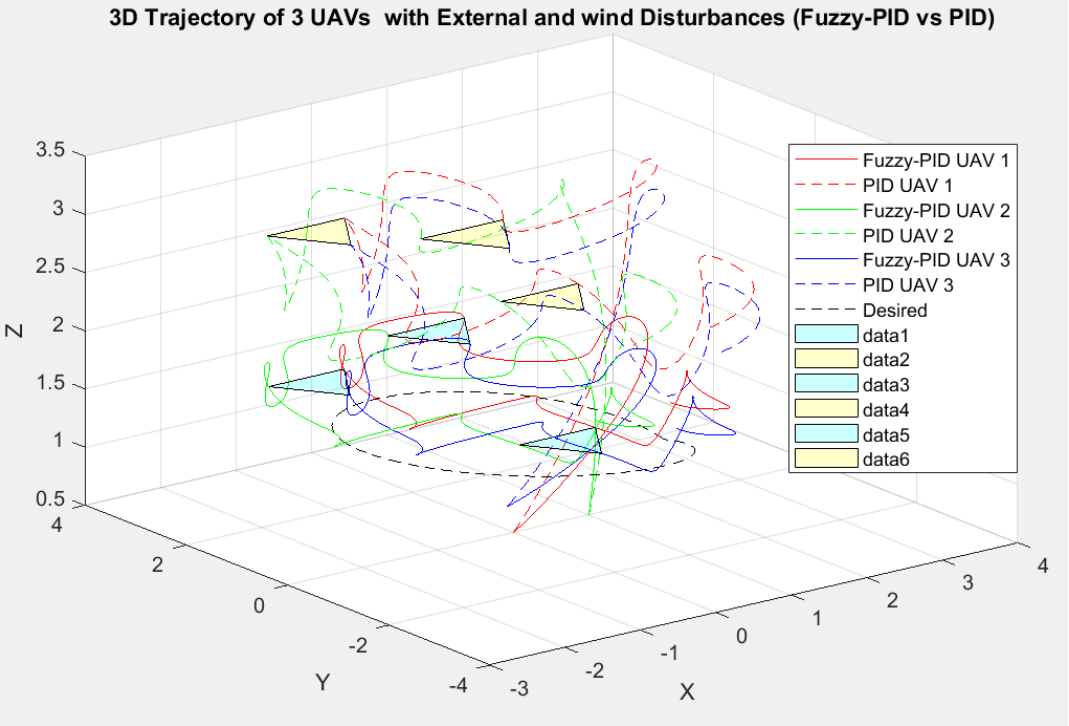

Figure 20. 3D position response x, y, z with triangular formation using fuzzy PID and PID controllers under wind and external disturbance.

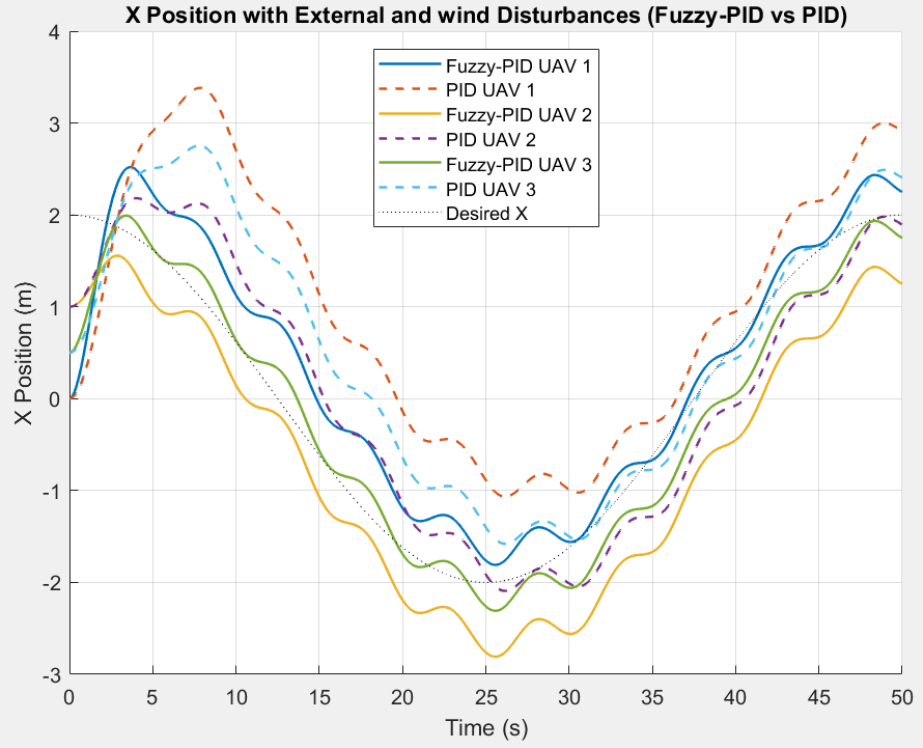

Figure 21. X position response with triangular formation using fuzzy PID and PID controllers under wind and external disturbance.

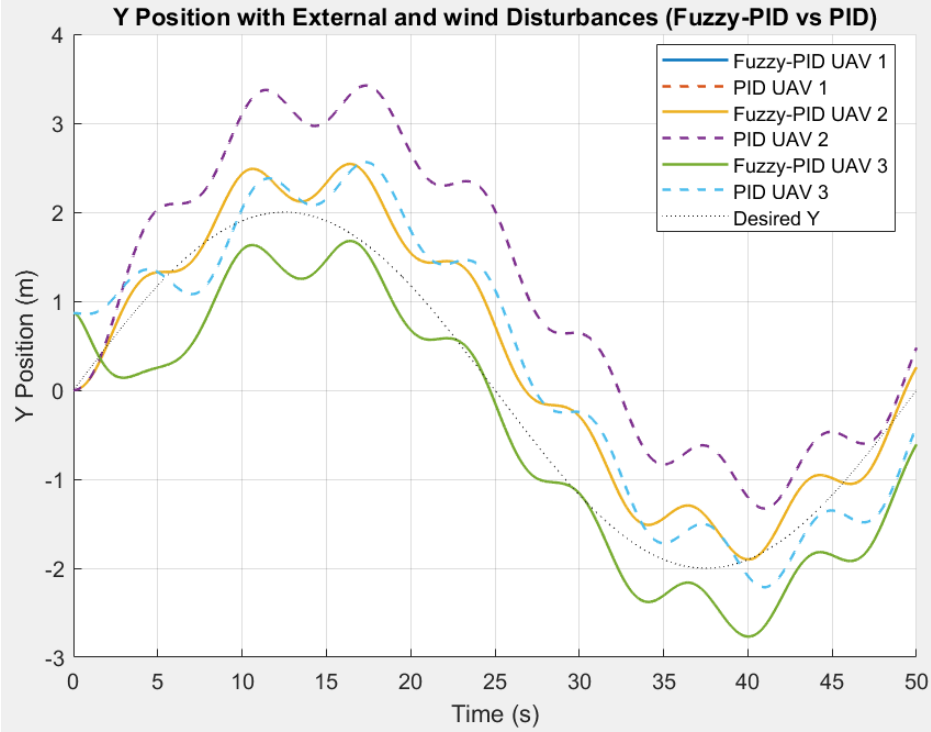

Figure 22. Y position response with triangular formation using fuzzy PID and PID controllers under wind and external disturbance.

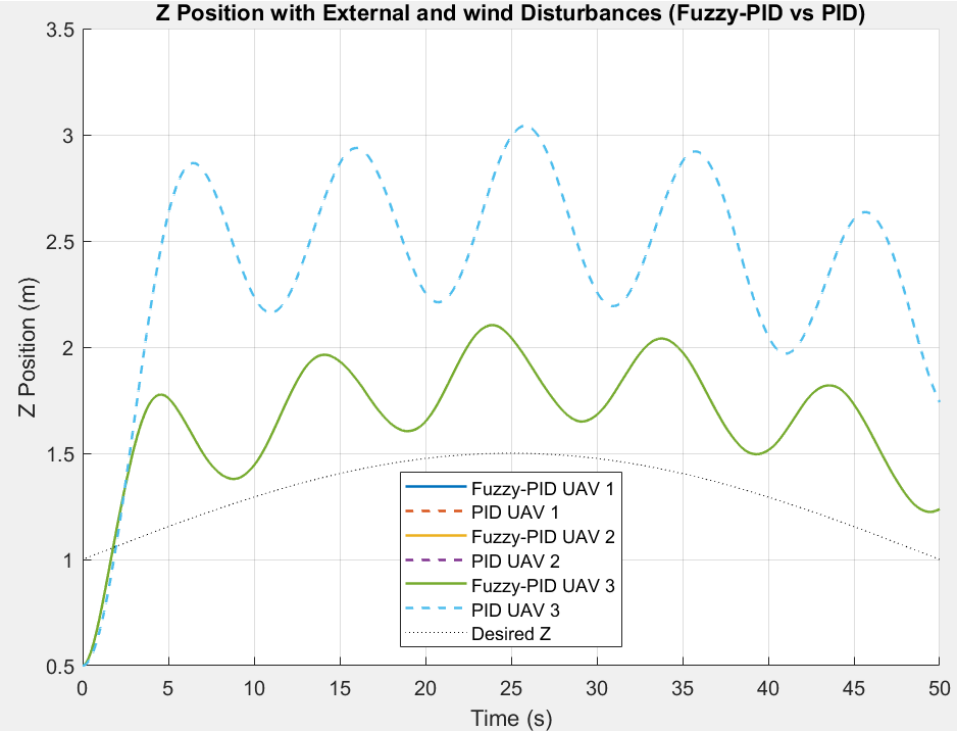

Figure 23. Z position response with triangular formation using fuzzy PID and PID controllers under wind and external disturbance.

Table 9 presents the results of a comparison of the average control performance metrics of three UAVs operating in a triangular formation under the influence of external noise and wind disturbance along the altitude axis. The results show that the fuzzy PID controller significantly outperforms the traditional PID controller on key criteria. The rise time decreases from 1.62 (PID) to 1.43 s (fuzzy PID), indicating faster response. At the same time, the overshoot percentage drops sharply from 204.83% to 110.55%, demonstrating better oscillation damping and improved system stability. Additionally, the steady-state error decreases from 0.7136 to 0.2245 m, confirming higher trajectory tracking accuracy. However, both controllers have equivalent settling times of 50.01 s, indicating that the long-term convergence process primarily depends on the system dynamics and noise conditions. These results highlight the effectiveness of the fuzzy PID method in enhancing control performance in uncertain environments.

Table 9. Evaluation of average quality control metrics for three UAVs in triangular formation altitude Z using fuzzy PID and PID controllers (wind and external disturbance conditions).

Formation / Quality index	Triangular formation (fuzzy PID)	Triangular formation (PID)
Rise time (s)	1.43	1.62
Steady time (s)	50.01	50.01
Overshoot (%)	110.55	204.83
Steady-state error (m)	0.2245	0.7136

Table 10. Quantitative comparison of control performance between PID and fuzzy PID controllers (wind and external disturbance conditions).

Quality index / Controller	MSE (PID)	MSE (fuzzy PID)	RMSE (PID)	RMSE (fuzzy PID)
X	0.911284	0.292970	0.9113	0.5250
Y	1.12453	0.257515	1.0166	0.5053
Z	1.331349	0.166584	1.1538	0.4081

Table 10 presents the results of a quantitative comparison of control quality between the traditional PID controller and the fuzzy PID controller under simultaneous external noise and wind disturbance conditions. The results show that fuzzy PID achieves lower MSE and RMSE values than PID across all three motion axes (x, y, and z). On the x-axis, MSE decreases from 0.911284 to 0.292970, corresponding to an improvement of approximately 67.85%, while RMSE decreases from 0.9113 to 0.5250. For the y-axis, MSE decreases from 1.12453 to 0.257515, representing an improvement of about 77.10%, and RMSE decreases from 1.0166 to 0.5053. The most significant improvement occurs on the z-axis, where MSE decreases from 1.331349 to 0.166584, equivalent to an improvement of approximately 87.49%, and RMSE decreases from 1.1538 to 0.4081. The simulation results demonstrate that the fuzzy PID controller achieves superior trajectory tracking accuracy and enhanced disturbance rejection performance compared to the conventional PID controller. In conditions with combined wind disturbance, MSE decreases by up to 87.49% along the z-axis, and RMSE decreases from 1.1538 to 0.4081, demonstrating superior disturbance rejection performance compared to the conventional PID controller. In particular, the substantial reduction in z-axis error indicates that the adaptive adjustment mechanism based on fuzzy inference is highly effective in altitude control, which is significantly affected by lift forces, aerodynamic disturbances, and wind effects.

The results from Figures 6-23 and Tables 3-10 provide a comprehensive evaluation of the UAV control system's performance under various operating conditions, showing that the fuzzy PID controller achieves superior trajectory tracking quality with smaller oscillations and shorter settling times compared to the traditional PID, particularly in environments with external noise and wind disturbance. Quantitative metrics such as overshoot, steady-state error, MSE, and RMSE are significantly improved, with the greatest improvement observed on the z-axis, reflecting good adaptability to nonlinear characteristics and environmental fluctuations. In combined noise scenarios, fuzzy PID maintains stable responses, while PID exhibits larger oscillations and higher cumulative errors. This result confirms the consistency between qualitative and quantitative analyses and demonstrates the effectiveness and applicability of the proposed method. Additionally, under the influence of wind disturbances and parameter uncertainty, the fuzzy inference mechanism serves as an adaptive nonlinear regulator, continuously updating the gain based on the system's state to enhance robustness and noise resistance. However, the system's performance still depends on the structure of the membership functions; thus, sensitivity analysis regarding parameters such as centroid position, width, and overlap will be conducted in future studies to optimize and ensure the long-term stability of the controller.

In addition, to evaluate the effectiveness of the controller, a systematic comparative analysis is conducted with nonlinear control strategies and typical formation control methods published in the literature [6–8,12,13,16,30–34], as summarized in Table 11. The analysis is based on four core criteria, namely (i) the completeness of the 6-DOF nonlinear dynamic model, (ii) the ability to

explicitly consider external disturbances in the design and evaluation of control, (iii) the existence of a theoretical stability analysis foundation, and (iv) the ability to implement within the geometric formation control structure.

Table 11. Comparative evaluation of representative UAV control strategies.

Ref.	Method	Full 6-DOF nonlinear model	Disturbance considered	Stability analysis	Formation control	Control complexity
[6]	Robust LQR	Partial	Yes	Yes	No	Medium
[7]	Nonlinear H∞	Yes	Yes	Yes	No	High
[8]	Fuzzy terminal SMC	Yes	Yes	Yes	No	High
[12], [13]	Fuzzy PID	Partial	Limited	No	No	Low
[16]	Distributed MPC	Yes	Yes	Yes	Yes	High
[30-34]	PID/MPC Formation	Mostly linearized	Limited	Partial	Yes	Medium-high
This study	Mamdani fuzzy PID formation	Yes	Yes (bounded external disturbances)	Simulation-based bounded response	Yes (triangular leader-follower)	Medium

The results presented in the previous sections indicate that the proposed Mamdani fuzzy PID controller provides significant improvements in transient performance and steady-state accuracy under both nominal conditions and when subjected to external disturbances. The system maintains bounded error and stable responses even under the influence of bounded noise, demonstrating the control structure's effective noise filtering capability. Compared to robust nonlinear control strategies such as H∞ [7] or sliding mode control [8], the proposed method achieves competitive performance in handling disturbances while significantly reducing computational complexity and parameter design requirements, thereby increasing feasibility for practical implementation. Additionally, formation control strategies based on distributed MPC [16], while advantageous for handling constraints and optimizing trajectories under uncertain conditions, often entail high computational costs and require continuous information exchange between agents. In contrast, the proposed leader–follower triangular formation structure in this study uses fixed geometric deviation vectors to simplify the coordination mechanism, reduce communication load, and maintain the geometric formation in the three-dimensional space. Furthermore, it is essential to note that many previous formation control works [30–34] primarily relied on linearized or partially nonlinear models and did not conduct comprehensive disturbance evaluations on the complete 6-DOF Euler–Lagrange dynamic model. In contrast, the current study explicitly considers the interplay between rotational and translational dynamics while integrating a model of bounded external noise into simulations and performance evaluation, thereby providing a more accurate analytical framework for real operational conditions. Overall, the comparative analysis shows that the proposed method achieves a reasonable balance between the accuracy of the nonlinear model, noise filtering capability, computational efficiency, and the ability to maintain geometric formation. This balance is particularly suitable for multi-agent UAV systems that require real-time deployment, given limited computational resources and communication infrastructure.

5. Conclusions

The paper proposes a triangular formation control method for UAVs based on a leader-follower structure, combined with a Mamdani fuzzy PID controller, on a fully nonlinear 6-DOF model. Simulation results indicate that the proposed method achieves superior performance compared to traditional PID controllers under various operating conditions. In noise-free conditions, fuzzy PID significantly improves response quality, reducing rise time from 3.29 to 2.03 s (~38%), decreasing overshoot from 55.74% to 50.30%, and lowering steady-state error from 0.0365 to 0.0315 m (~13.7%). Additionally, MSE and RMSE metrics show significant reductions, especially on the z-axis, with MSE decreasing by over 56.9%, demonstrating improved trajectory tracking accuracy. Under external noise conditions, fuzzy PID exhibits strong noise suppression capabilities, reducing overshoot from 227.50% to 88.58% (~61%) and steady-state error from 1.0272 to 0.4060 m (~60.5%). MSE decreases by up to 88.8% on the z-axis, indicating good adaptability to environmental disturbances. In conditions with combined external noise and wind disturbance, performance continues to improve significantly, with MSE decreasing from 1.331349 to 0.166584 (~87.49%) and RMSE decreasing from 1.1538 to 0.4081 on the z-axis. Simultaneously, overshoot decreases from 204.83% to 110.55%, and steady-state error decreases from 0.7136 to 0.2245 m, demonstrating the ability to maintain stability and accurate trajectory tracking in complex real-world environments. Quantitative results show that the fuzzy PID controller not only significantly improves trajectory tracking quality but also enhances the robustness, noise resistance, and stability of the formation UAV system. The proposed method achieves an effective balance between control accuracy, computational complexity, and practical applicability, making it particularly suitable for multi-agent UAV systems operating in uncertain environments.

In the future, this research will be expanded in several key directions to enhance both theoretical rigor and practical applicability. First, a rigorous stability analysis based on Lyapunov theory will be developed to provide mathematical guarantees for the closed system. Next, the proposed control method will be validated through experimental implementation on real UAV platforms. At the same time, the methodological framework will be extended for multi-UAV systems with a more flexible formation structure, incorporating advanced functions such as obstacle avoidance and adaptive noise estimation. Additionally, practical factors of the communication channel in the leader-follower structure, including transmission delays, packet loss, and asynchronous information updates, will be systematically examined. Furthermore, comparative studies with advanced nonlinear and optimal control methods, such as model predictive control (MPC) and adaptive backstepping, will be conducted to clarify performance trade-offs.

Use of Generative-AI tools declaration

The authors declare they have not used Artificial Intelligence (AI) tools in the creation of this article.

Conflict of interest

The authors declare there is no conflict of interest in this paper.

References

1. Zhao S, Lu K, Wu S, Su D (2021) Helicopter Flight Dynamics Modeling Using Simulink. *2021 33rd Chinese Control and Decision Conference (CCDC*), 2591–2596. https://doi.org/10.1109/CCDC52312.2021.9601647
2. Abdelhaya S, Zakriti A (2019) Modeling of a Quadcopter Trajectory Tracking System Using PID controller. *Procedia Manufacturing* 32: 564–571. https://doi.org/10.1016/j.promfg.2019.02.253
3. Zhou X, Yu X, Guo K, Zhou S, Guo L, Zhang Y, et al. (2023) Safety Flight Control Design of a Quadrotor UAV With Capability Analysis. *IEEE T Cybernetics* 53: 1738–1751. https://doi.org/10.1109/TCYB.2021.3113168
4. Mien TL, Tu TN, An VV (2024) Cascade PID Control for Altitude and Angular Position Stabilization of 6-DOF UAV Quadcopter. *International Journal of Robotics and Control Systems* 4: 814–831. https://doi.org/10.31763/ijrcs.v4i2.1410
5. Mien TL, Van An V (2024) Modeling and control of 6-DOF UAV quadcopter using PID controllers arcording to Ziegler-Nichols. *III International Scientific and Practical Conference «Intelligent Transport Systems», Moscow*, 438–492. https://doi.org/10.30932/9785002446094-2024-483-492
6. Elkhatem AS, Engin SN (2022) Robust LQR and LQR-PI control strategies based on adaptive weighting matrix selection for a UAV position and attitude tracking control. *Alex Eng J* 61: 6275–6292. https://doi.org/10.1016/j.aej.2021.11.057
7. Raffo GV, Ortega MG, Rubio FR (2010) An integral predictive/nonlinear H∞ control structure for a quadrotor helicopter. *Automatica* 46: 29–39. https://doi.org/10.1016/j.automatica.2009.10.018
8. Nekoukar V, Dehkordi NM (2021) Robust path tracking of a quadrotor using adaptive fuzzy terminal sliding mode control. *Control Eng Pract* 110: 104763. https://doi.org/10.1016/j.conengprac.2021.104763
9. Housny H, Chater EA, El Fadil H (2019) New Deterministic Optimization Algorithm for Fuzzy Control Tuning Design of a Quadrotor. *2019 5th International Conference on Optimization and Applications (ICOA),* 1-6. https://doi.org/10.1109/ICOA.2019.8727622
10. Van AV, Duy HH (2025) Control Strategies for 6-DOF Quadcopter UAVs: Cascade PID Stabilization in White Noise Conditions. *Makara J Technol* 29: 119–132. https://doi.org/10.7454/mst.v29i3.1697
11. Van An V, Mien TL, Van Binh N Vo (2026) A comprehensive survey of UAV control algorithms: Integrating classical methods with artificial intelligence for enhanced trajectory tracking. *AIMS Electronics and Electrical Engineering* 10: 26–53. https://doi.org/10.3934/electreng.2026002
12. Sheng G, Gao G (2019) Research on the Attitude Control of Civil Quad-Rotor UAV Based on Fuzzy PID Control. *2019 Chinese Control And Decision Conference (CCDC)*, 4566–4569. https://doi.org/10.1109/CCDC.2019.8832855
13. Jiang M (2021) Application of Fuzzy PID Control in UAV Control System. *2021 Third International Conference on Inventive Research in Computing Applications (ICIRCA)*, 197–200. https://doi.org/10.1109/ICIRCA51532.2021.9544986
14. Yang S, Xian B (2020) Exponential Regulation Control of a Quadrotor Unmanned Aerial Vehicle With a Suspended Payload. *IEEE T Contr Syst Tech* 28: 2762–2769.

15. Castillo P, Lozano R, Dzul A (2005) Stabilization of a mini rotorcraft with four rotors. *IEEE Contr Syst Mag* 25: 45–55. https://doi.org/10.1109/MCS.2005.1550152
16. Luis CE, Vukosavljev M, Schoellig AP (2020) Online Trajectory Generation With Distributed Model Predictive Control for Multi-Robot Motion Planning. *IEEE Robot Autom Lett* 5: 604–611. https://doi.org/10.1109/LRA.2020.2964159
17. Labbadi M, Boukal Y, Cherkaoui M, Djemai M (2021) Fractional-order global sliding mode controller for an uncertain quadrotor UAVs subjected to external disturbances. *Journal of the Franklin Institute* 358: 4822–4847. https://doi.org/10.1016/j.jfranklin.2021.04.032
18. Karahan M, Inala M, Kasnakoglu C (2023) Fault Tolerant Super Twisting Sliding Mode Control of a Quadrotor UAV Using Control Allocation. *International Journal of Robotics and Control Systems* 3: 270–285. https://doi.org/10.31763/ijrcs.v3i2.994
19. Daadi A, Boulebtinaia H, Derrouaouia SH, Boudjema F (2022) Sliding Mode Controller Based on the Sliding Mode Observer for a QBall 2+ Quadcopter with Experimental Validation. *International Journal of Robotics and Control Systems* 2: 332–356. https://doi.org/10.31763/ijrcs.v2i2.693
20. Mobarez EN, Sarhan A, Ashry M (2019) Fractional order PID Based on a Single Artificial Neural Network Algorithm for Fixed wing UAVs. *2019 15th International Computer Engineering Conference (ICENCO),* 1–7. https://doi.org/10.1109/ICENCO48310.2019.9027378
21. Sahrir NH, Basri AM (2024) Radial Basis Function Network Based Self-Adaptive PID Controller for Quadcopter. *International Journal of Robotics and Control Systems* 4: 151–173. https://doi.org/10.31763/ijrcs.v4i1.1261
22. Ma'arif A, Suwarno I, Nur'aini E, Raharja NM (2023) Altitude Control of UAV Quadrotor Using PID and Integral State Feedback. *BIO Web of Conferences* 65: 07011. https://doi.org/10.1051/bioconf/20236507011
23. Shamrooz S, Aslam MS, Liu H, Bilal H, Vasilakos AV (2025) Modeling of Asynchronous Mode-Dependent Delays in Stochastic Markovian Jumping Modes Based on Static Neural Networks for Robotic Manipulators. *IEEE T Autom Sci Engi* 22*:* 13398–13410.
24. Bilal H, Rehman A, Aslam MS, Ullah I, Chang WJ, Kumar N, et al. (2025) Hybrid TrafficAI: A Generative AI Framework for Real-Time Traffic Simulation and Adaptive Behavior Modeling. *IEEE T Intell Transp Syst* 99: 1–17. https://doi.org/10.1109/TITS.2025.3571041
25. Bilal H, Obaidat MS, Aslam MS, Zhang J, Yin B, Mahmood K (2024) Online Fault Diagnosis of Industrial Robot Using IoRT and Hybrid Deep Learning Techniques: An Experimental Approach. *IEEE Internet Things* 11: 31422–31437. https://doi.org/10.1109/JIOT.2024.3418352
26. Aslam MS, Bilal H, Vasilakos AV (2025) Self-Triggered Scheme Design for Takagi-Sugeno Fuzzy Model Based on Mismatch Premise Variable With Time-Varying Delay. *IEEE T Autom Sci Eng* 22: 15536–15548. https://doi.org/10.1109/TASE.2025.3570089
27. Aslam MS, Bilal H, Chang W, Kumar N, Khan IA, Vasilakos AV (2025) H∞ Delayed Filtering of Markov Jump Fuzzy Systems in Consumer Electronics: Input–Output Analysis. *IEEE T Consum Electron* 71: 7002–7013. https://doi.org/10.1109/TCE.2025.3565105
28. Hussan U, Waheed A, Bilal H, Wang H, Hassan M, Ullah I, et al. (2025) Robust Maximum Power Point Tracking in PV Generation System: A Hybrid ANN-Backstepping Approach With PSO-GA Optimization. *IEEE T Consum Electron* 71: 6016–6026. https://doi.org/10.1109/TCE.2025.3569871

29. Ullah R, Bilal H, Aslam MS, Ayouni S, Majid A, Vasilakos AV, et al. (2026) Conformer-PhyFaultNet: Physics-Informed Spectral Attention Conformer for Generalizable Bearing Fault Diagnosis. *IEEE Internet Things* 99: 1–15. https://doi.org/10.1109/JIOT.2026.3662413
30. Chen Y, Deng T (2023) Leader-Follower UAV formation flight control based on feature modeling. *Systems Science & Control Engineering: An Open Access Journal* 11: 2268153.
31. Shafiq M, Khan AM (2022) Formation control of multiple UAVs using PID control approach. *Int J Model Identif Contr* 39: 340–349.
32. Rafifandi R, Asri DL, Ekawati E, Budi EM (2019) Leader–follower formation control of two quadrotor UAVs. *SN Applied Sciences* 1: 539.
33. Konatowski S, Tatko S (2023) Behaviour of unmanned aircraft in formation. *Przegląd Elektrotechniczny* 99: 53–58.
34. Ghaderi F, Toloei A, Ghasemi R (2024) Formation Control and Obstacle Avoidance of a Multi-Quadrotor System Based on Model Predictive Control and Improved Artificial Potential Field. *International Journal of Engineering, Transactions A: Basics* 37: 115–126.
35. Le Thi Thu Ha (2018) Thiet Ke Bo Dieu Khien Thich Nghi PID Nho Suy Luan Mo Va Ung Dung Cho He Truyen Dong Qua Banh Rang. *Tap Chi Khoa Hoc va Cong Nghe* 176: 179–184.
36. Surriani A, Budiyanto MU, Arrofiq M (2017) Altitude Control of Quadrotor using Fuzzy Self Tuning PID Controller. *2017 5th International Conference on Instrumentation, Control, and Automation (ICA)*, 67–72. https://doi.org/10.1109/ICA.2017.8068415
37. Sharma M, Sakthivel R, Yadav K (2026) Distributed event-triggered robust adaptive formation control of multi agent rigid bodies on $TSE(3)^N$. *Sci Rep*. https://doi.org/10.1038/s41598-026-47678-1
38. Vera-Amaro R, Luviano-Juárez A, Rivero-Ángeles ME (2026) Delay-Aware UAV Swarm Formation Control via Imitation Learning from ARD-PF Expert Policies. *Drones* 10: 34. https://doi.org/10.3390/drones10010034
39. Farooq A, Xiang Z, Chang WJ, Aslam MS (2025) Recent Advancement in Formation Control of Multi Agent Systems: A Review. *Computers, Materials and Continua* 83: 3623–3674. https://doi.org/10.32604/cmc.2025.063665

AIMS Press